Li *et al. Earth, Planets and Space* (2017) 69:27
DOI 10.1186/s40623-017-0610-x

Earth, Planets and Space

FULL PAPER

Open Access

Dynamics of the Wulong landslide revealed by broadband seismic records

Zhengyuan Li[1], Xinghui Huang[1*], Qiang Xu[2], Dan Yu[1], Junyi Fan[1] and Xuejun Qiao[3]

Abstract

The catastrophic Wulong landslide occurred at 14:51 (Beijing time, UTC+8) on 5 June 2009, in Wulong Prefecture, Southwest China. This rockslide occurred in a complex topographic environment. Seismic signals generated by this event were recorded by the seismic network deployed in the surrounding area, and long-period signals were extracted from 8 broadband seismic stations within 250 km to obtain source time functions by inversion. The location of this event was simultaneously acquired using a stepwise refined grid search approach, with an error of ~2.2 km. The estimated source time functions reveal that, according to the movement parameters, this landslide could be divided into three stages with different movement directions, velocities, and increasing inertial forces. The sliding mass moved northward, northeastward and northward in the three stages, with average velocities of 6.5, 20.3, and 13.8 m/s, respectively. The maximum movement velocity of the mass reached 35 m/s before the end of the second stage. The basal friction coefficients were relatively small in the first stage and gradually increasing; large in the second stage, accompanied by the largest variability; and oscillating and gradually decreasing to a stable value, in the third stage. Analysis shows that the movement characteristics of these three stages are consistent with the topography of the sliding zone, corresponding to the northward initiation, eastward sliding after being stopped by the west wall, and northward debris flowing after collision with the east slope of the Tiejianggou valley. The maximum movement velocity of the sliding mass results from the largest height difference of the west slope of the Tiejianggou valley. The basal friction coefficients of the three stages represent the thin weak layer in the source zone, the dramatically varying topography of the west slope of the Tiejianggou valley, and characteristics of the debris flow along the Tiejianggou valley. Based on the above results, it is recognized that the inverted source time functions are consistent with the topography of the sliding zone. Special geological and topographic conditions can have a focusing effect on landslides and are key factors in inducing the major disasters, which may follow from them. This landslide was of an unusual nature, and it will be worthwhile to pursue research into its dynamic characteristics more deeply.

Keywords: Wulong landslide, Broadband seismic signals, Source time functions, Dynamic landslide process

Background

A massive landslide occurred at 14:51 (Beijing time, UTC+8) on 5 June 2009, in Wulong prefecture, Chongqing, claiming 74 lives and injuring 8 others. The landslide caused permanent damage to the local environment, and huge losses to local people (Xu et al. 2009). Geological surveys show that the landslide started with a lateral slump of the bedrock on the upper part of the cliff over the west slope of the Tiejianggou valley. Rocks became detached and fell from the near-vertical cliff with a height of around 50 m, acquiring a very high speed. A raised slope in front was destroyed; sediments and underlying bedrock were completely scoured. Large amounts of broken rocks and debris crossed the 200 m wide and 50 m deep Tiejianggou valley, colliding with the east slope of the valley at a very high speed. Blocked by the slope, the high-speed projectiles and crushed rock collided, spilled, and rolled. The material then flowed downstream along the terrain, forming a 30 m thick and 2200 m long accumulation area. Topographic measurements before and after the landslide show that the volume was approximately 5×10^6 m^3 at the beginning, and

*Correspondence: huangxh19850216@gmail.com
[1] China Earthquake Networks Center, Beijing 100045, China
Full list of author information is available at the end of the article

became 7×10^6 m^3 by the end of the landslide, due to the expansion of mass during collisions and entrainments of sedimentary materials during sliding (Xu et al. 2009; Yin 2010).

Massive landslides are catastrophic natural geological hazards that pose a considerable threat to residents of mountain areas. Systematic research on their development and occurrence is very important for early warnings and disaster prevention, yet it requires a large amount of quantitative observations. However, it is not easy to deploy detectors for quantitative observations before a landslide, due to their unpredictability. Moreover, massive landslides are usually very destructive; even if detectors are deployed before the event, they may be destroyed by it. The lack of direct observations is an obstacle to the better understanding of massive landslides.

Seismic networks can provide quantitative observations for vibrations of the ground surface generated by remote seismic sources, commonly earthquakes, but also volcanoes and landslides. Their remoteness ensures the integrity and continuity of the observations, as the equipment is not destroyed by the events being monitored. The quantitative nature of seismic records can be used to extract the dynamic parameters of the seismic sources (landslides in this case), making up for the lack of field observations. Recent studies have shown that the extraction and analysis of seismic network data can explain the linchpin process and mechanism of landslides, especially their geological characteristics (Lin 2015; Petley 2013); providing quantitative data for determining key timings, tracing back processes, and analyzing potential risks. Seismic radiations from landslides consist of short-period signals, resulting from collisions between blocks and sliding boundaries, and long-period signals, generated by the unloading and reloading of the Earth's crust. Correspondingly, two approaches have been developed for research on landslides using seismic signals. The first approach uses the short-period signals, usually for spectral analysis and qualitative descriptions; the second approach involves calculating source time functions of the landslide using inversions of long-period seismic records (Ekström and Stark 2013; Hibert et al. 2014, 2015; Lin et al. 2010; Yamada et al. 2013; Zhao et al. 2015). In this paper, long-period signals extracted from 8 broadband seismic stations within 250 km of the Wulong landslide are used to determine its source time functions. Combining this data with topographic surveys done before and after the event, we analyze the different stages of the landslide movement from its kinematic parameters, calculate the basal friction coefficients for each stage, and discuss the relationship with the topography.

The Wulong landslide

Jiwei Mountain, where the Wulong landslide occurred, is located in southwest China. Geological hazards happen frequently in this area, especially during rainy seasons, because of the steep slopes, deep valleys, and loose vegetation. Research shows that the unstable geological setting was a precondition of this landslide; karstifications and mining activities were the main affecting factors; and failure of the key block triggered the landslide (Xu et al. 2009). Fissures at the top of the cliff, the source zone of the landslide, were discovered more than 40 years ago, indicating a long-term separation of the column from Jiwei Mountain. This unstable structure was observed and researched after being discovered, and scientists provided pre-event warnings to the local government before the landslide. A photograph taken immediately before the event is shown in Additional file 1: Figure S1. In the photo, a key block which supported the bulk of the landslide material for a very long time can be clearly seen, along with the stable bedrock, and loose material which was scoured during the landslide (Xu et al. 2009). This was a rock landslide, which released enormous energy in a very short time. The topography was permanently changed, and the environment and life of the local residents were greatly affected.

After the Wulong landslide, a professional group, supported by the Ministry of Land and Resources of the People's Republic of China and the State Administration of Work Safety, carried out a field investigation (Xu et al. 2009). Generally speaking, the landslide region consists of a source zone and a depositional zone. The depositional zone can be further divided into a scouring zone, a main depositional zone, a debris depositional zone, and a scatter zone, as shown in Fig. 1. Special geological and topographic conditions are key factors in inducing major disasters. The main depositional zone and the debris depositional zone distributed material along the Tiejianggou valley from south to north. The source zone is located on the west cliff of the Tiejianggou valley, about 600 m higher than the depositional zones, providing major kinetic energy to the sliding mass. The strike of the free face of the cliff is around 8°, approximately parallel to the Tiejianggou valley. The major sliding mass was originally the upper part of the cliff, yet this detached and fell, leaving a sliding surface with a dip of around 21° and an inclination direction of approximately 345°, toward the inside of the mountain. It could be inferred from the geological setting of the source area that during the initiation stage of the landslide, the mass moved approximately northward on the sliding surface, as shown in Fig. 1. For a very long time before the landslide, the mass retained its stability due to the key block in front, shown in Additional file 1: Figure S1; but the stress was constantly accumulating

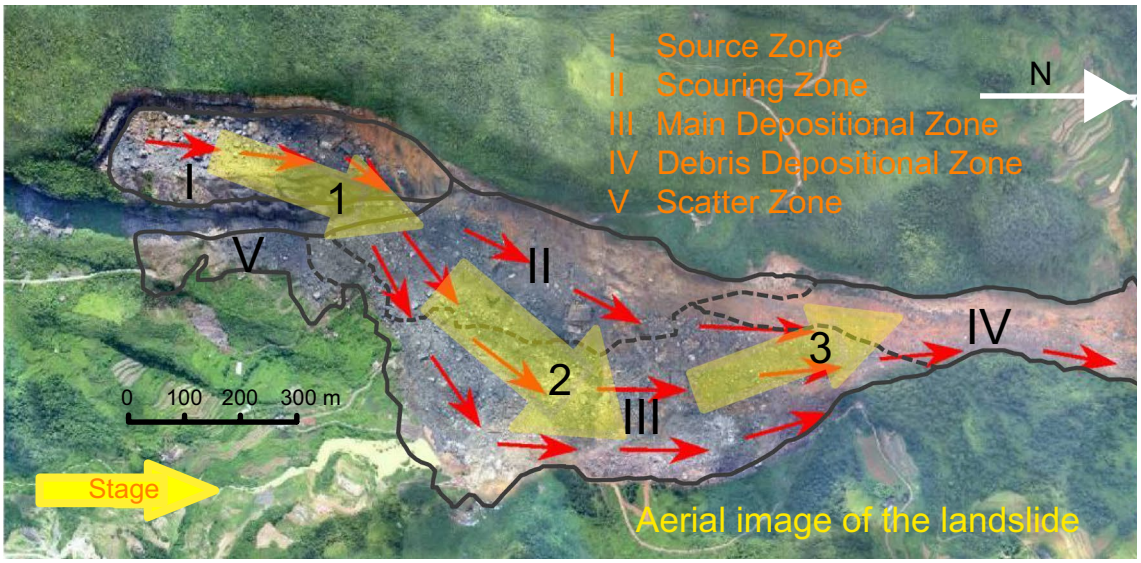

Fig. 1 The aerial image after the landslide. *Red lines* with *arrows* depict the path of the landslide; *gray solid lines* depict the spatial ranges of the landslide area; *gray dashed lines* depict Zones I–V; the three stages recognized from estimated source time functions are also depicted using semi-transparent *yellow arrows*

under the effect of gravity. The failure of the key block triggered this massive landslide. Being stopped by the stable bedrock in front, the mass changed its direction of movement to the east, forming the scouring zone (II in Fig. 1). The mass ran down the west slope of the Tiejianggou valley, acquiring a large amount of kinetic energy, and crossed the valley bottom at a very high speed, colliding with the east slope of the valley. The mass broke up into small pieces as a result of the collision, and flowed along the valley, forming the main depositional zone (III in Fig. 1) and the debris depositional zone (IV in Fig. 1). Additional file 2: Figure S2 is a photograph taken after the landslide, showing small pieces of rock. Tiejianggou is a long, narrow, and closed, inclined guide valley. The debris frequently collided with the boundaries of the valley while flowing. Energy and material gathered within the valley and had no means of diffusing, which was in part responsible for the major disaster. The source zone is on the top of the cliff, around 50 m higher than the west slope. During the initiation stage, a large amount of rock was scattered from the free side of the cliff, forming the scatter zone (V in Fig. 1).

Seismic observations

A total of 36 seismic stations are deployed by the China Earthquake Networks Centers (CENC) within the 400 km range of the Wulong landslide, and their locations are shown in Fig. 2. The network detected an event, which occurred on the same day as the landslide, and with a location very close to it. (Our inversion results, provided in later sections, also show that the location of the event detected by the network was close to the landslide). In addition, the characteristics of the seismic signals are different from those generated by earthquakes, and there was no earthquake of a similar magnitude reported within the relevant area. Thus, we can confirm that the seismic event was generated by this landslide.

Most of the seismometers deployed in the relevant area detected this event, but not all of the seismic records were suitable for inversion. We first screened out those seismic signals recorded by a narrow frequency band seismometer and then chose the seismic records, which qualified for the inversion from the rest. We compared background signals (before and after the event) with effective signals (containing the event) to rule out seismic signals without apparent effective energy in the target frequency band. An example is provided in Additional file 3: Figure S3. We selected 15 sets of seismic records from 8 broadband seismic stations to do the inversion. The other 9 sets of seismic records from the 8 selected seismic stations were not suitable for the inversion, either because they contained large-amplitude low-frequency drafts (N-S component of WAS and U-D component of ROC) or because the effective signals could not be distinguished from the background signals in the target frequency band (U-D component of FUL, WAS and XCH; E-W component of CHS, QIJ and ROC; N-S component of XCH).

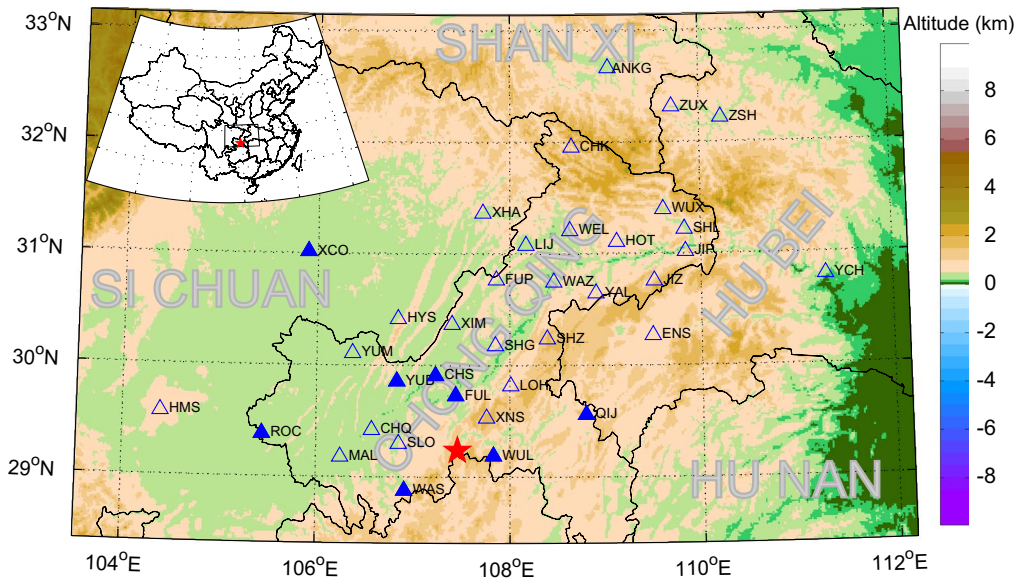

Fig. 2 Locations of the Wulong landslide (*red star*) and seismic stations (*blue triangles*). Seismic stations marked using a *solid triangle* were used in this inversion

Long-period signals were extracted from the selected broadband seismic records for the inversion of the source time functions, using the following procedure: first, the instrumental response was removed from each record to acquire the displacement; second, the seismic data were resampled to 0.2 s; and lastly, the seismic data were band-pass-filtered using a frequency band of 0.02–0.065 Hz. We chose this frequency band in the inversion to characterize the main stages of the landslide, since the entire event lasted around 1½ min, including three scenarios, which gives a time scale for each scenario in tens of seconds.

Methods

Seismometers are deployed on the surface of the Earth to record vibrations generated by faraway sources, which are propagated in the form of seismic waves. Therefore, seismic records contain information on the seismic source and can be used to retrieve its dynamic properties. The seismic source of a landslide satisfies a single force model, and the force acting on the crust is equivalent to the inertial force of the sliding mass (Kanamori and Given 1982; Kawakatsu 1989). It is normal to use the seismic records generated by a landslide to obtain source time functions through inversion.

The inversion is based on the assumption that the spatial range of the landslide should be small compared with the distance between the seismic stations and the event, since the method treats the landslide seismic source as a time-varying point force. Also, the wavelength of the seismic signals used in the inversion must be long enough to represent the unloading and reloading processes of the elastic crust resulting from the movement of the landslide. Basically, the inverted forces are those that act on the crust of the Earth. According to the action-reaction law, the forces acting on the sliding mass can be easily calculated by simply multiplying by −1.

The method for the inversion has been well developed in recent decades (Allstadt 2013; Nakano et al. 2008). For a landslide with given locations of seismic stations, theoretical seismic records can be expressed as follows:

$$s_m(j\Delta t) = \sum_{i=1}^{3}\sum_{l=1}^{nt} G_{im}(j\Delta t - l\Delta t) f_i(l\Delta t)\Delta t$$

where Δt is time sample rate, $s_m(j\Delta t)$ is the mth seismic record, $f_i(l\Delta t)$ is the ith component source, and $G_{im}(j\Delta t - l\Delta t)$ is the Green's Function of $f_i(l\Delta t)$ to $s_m(j\Delta t)$, i.e., the mth component of the seismic records generated by the ith force. The seismic records could be stated as the convolution of the source time functions with Green's Functions. Inversion is the opposite process, deconvolving the source time functions from the seismic records. To improve calculation stability, inversion uses as many seismic stations as possible. In this study, Green's Functions are calculated using a matrix propagation method (Wang 1999); the velocity model is derived from Crust1.0. For a given location, Crust 1.0 can provide a horizontal layered velocity model, including the 8 layers of water, ice, upper sediments, middle sediments,

lower sediments, upper crystalline crust, middle crystalline crust, and lower crystalline crust. For each layer, VP (P—wave velocity), VS (S—wave velocity) and rho (density) are provided with a horizontal resolution of 1° × 1° (http://igppweb.ucsd.edu/~gabi/crust1.html). In calculating Green's Functions, we removed the water, ice and upper sediments layers from the velocity model extracted from Crust1.0. We calculated Green's Functions at source nodes, shown in Fig. 3 using black points, to determine the best-fit location of the landslide.

Results and discussion

To improve computational efficiency, the inversion was carried out in the frequency domain. The best-fit source location, acquired using a refined grid search method, is shown in Fig. 3 with an error of ~2.2 km. A residual contour is also provided to show that the inversion is gradually converging in the selected region. Synthetic and recorded seismic signals are shown in Fig. 4. They fit very well, ensuring the validity of the inversion results. Seismic data sets with synthetic seismic waveforms shown as red dashed lines were not used in the inversion. We calculated source time functions of the sliding mass from the inversion results, based on the action-reaction law, and provide them in Fig. 5, with positive directions upward, eastward and northward, respectively. We interpret the source time functions as representing the three stages of this landslide, i.e., northward movement after initiation, eastward sliding after being blocked, and debris flow after collision with the east slope of the Tiejianggou valley (see 1–3 in Fig. 5).

In the first stage (80–108 s), the mass moved northward along the strike of the free side of the cliff; hence, the inertial force acting on the mass increased northward and downward. The force in the E-W direction was almost negligible. 86 s later, the sliding mass began to be blocked by the key block in front; the northward and downward forces started decreasing; still no apparent force appeared in the E-W direction. The northward and downward forces gradually decreased to zero and increased in the opposite directions. Failure of the key block occurred at approximately 98 s, stopping the increase of the upward and southward forces. Meanwhile, the westward inertial force started to increase, indicating westward movement of the sliding mass in the direction of the inclination of the sliding surface. This process lasted only around 10 s before the mass was blocked by the stable west side walls. In the second stage (108–137 s), the northward and westward movement of the mass was blocked by the stable side walls in front, redirecting it eastward, and leaving the scouring zone on the west wall (II in Fig. 1). Meanwhile, the mass fell from the cliff, sliding eastward along the west slope of the Tiejianggou valley. Accordingly, from 108 to 123 s, the westward force rapidly decreased

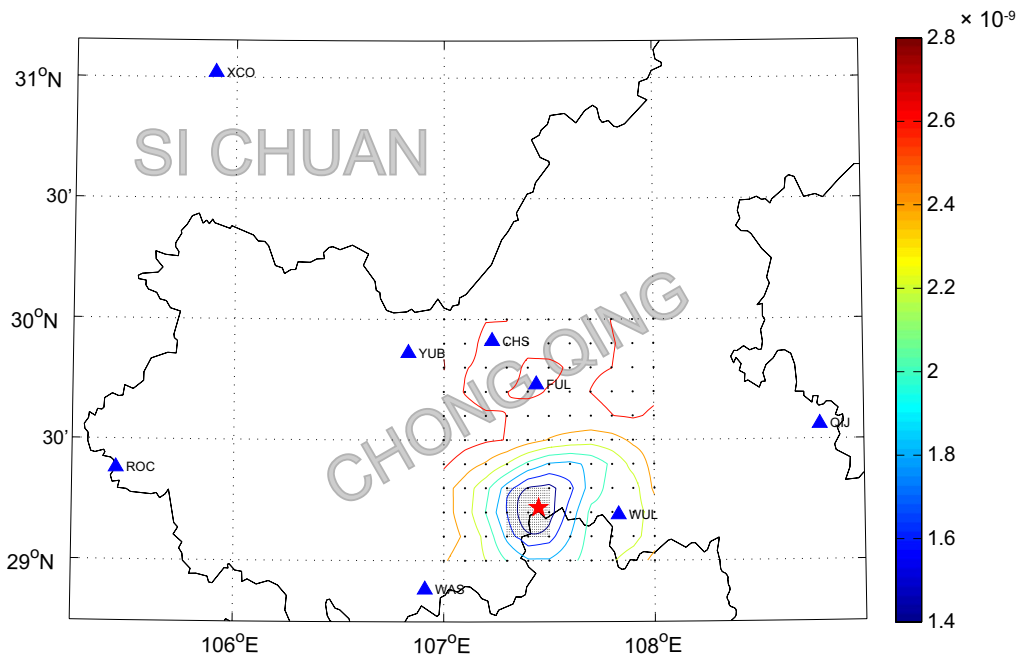

Fig. 3 Contour lines of inversion residuals, and seismic stations used in the inversion (*blue triangles*). The *dots* represent locations at which the Green's Functions were calculated

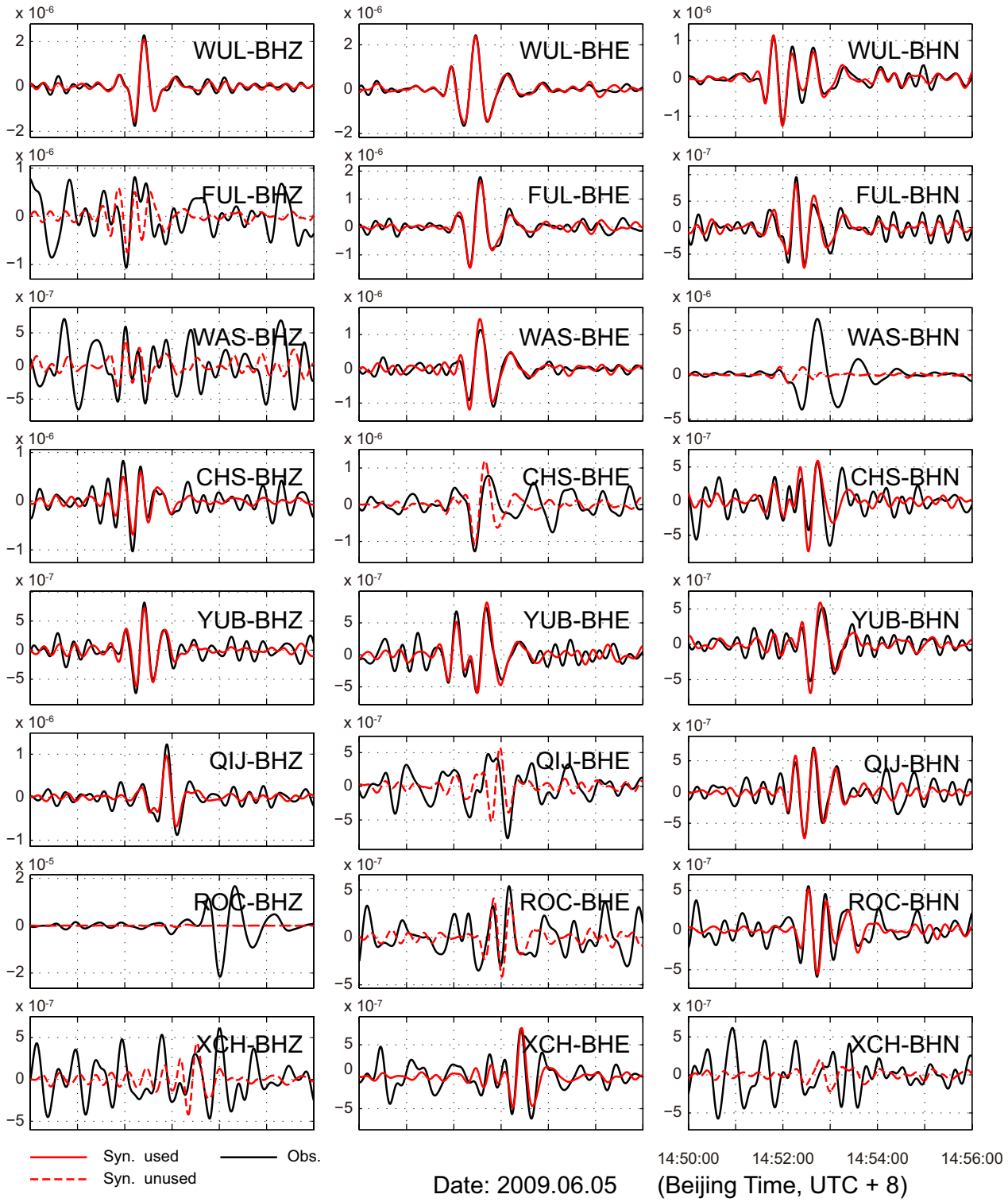

Fig. 4 Synthetic (*red lines*) and recorded (*black lines*) seismic signals. Seismic data sets with synthetic seismic waveforms, drawn using *red dashed lines*, were not used in the inversion. The *vertical axis* indicates displacement in meters

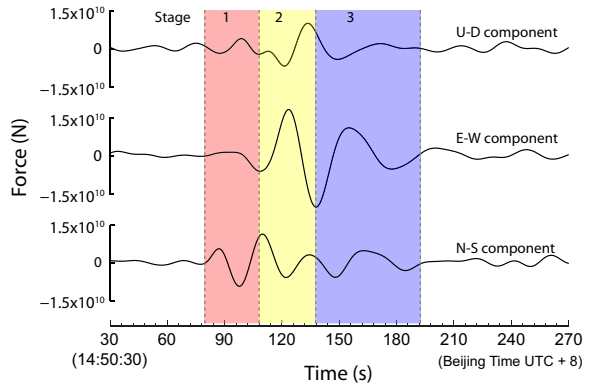

Fig. 5 Inverted source time functions of the Wulong landslide, representing three stages of the landslide, labeled 1–3

to zero and then increased to an eastward peak value; the northward force decreased to zero, and no longer dominated the movement; and the downward force reached its peak at around 123 s, showing similar characteristics to the eastward force. After 123 s, the eastward and downward forces started to decrease to zero and then reverse, reaching peak values in the opposite directions at around 137 s, indicating deceleration of the sliding mass and collision with the opposite side of the valley. In the third stage (137–192 s), the sliding mass broke up into small pieces after the collision with the east slope of the Tiejianggou valley. Detritus rebounded and oscillated between the boundaries of the valley, and flowed along the Tiejianggou valley, expending the previously collected kinetic energy. The sliding mass was deposited during this process, with the grain size sorting from large to small, forming the main depositional zone (III in Fig. 1) and the debris depositional zone (IV in Fig. 1). The estimated inertial force of the mass in the E-W direction exhibits oscillations and gradually decreased to zero at the end. The inertial force in the U-D component was negligible, indicating no apparent height differences along the Tiejianggou valley. A small, oscillating force could be detected in the N-S direction, revealing accelerations and decelerations of the mass in the debris flow.

The three stages revealed by the estimated source time functions are consistent with the topography of the landslide area. The corresponding areas are depicted in Fig. 1 using semi-transparent yellow arrows. The source of the landslide was the upper part of the cliff, consisting of extremely thick limestone that was cut into regular blocks by two near-vertical surfaces, approximately perpendicular with each other. A thin, weak layer developed along the sliding surface. Driven by gravity, the inclined plate-like limestone, which was also the source of the landslide, crept along the sliding surface long before the landslide occurred. The sliding surface inclined toward the northwest; but the mass could not go in this direction due to the stable mountain in front. Instead, the mass moved along the strike of the free side of the cliff, squeezing the key block in front. The shear force at the key block accumulated with time until the failure occurred, triggering the chain sliding disaster. Karstifications and mining activities also played important roles in this process. At the initiation of the landslide, the sliding mass moved along the free side of the cliff, almost exactly northward (see Stage 1 in Fig. 1). Estimated source time functions show that the force of the N-S component was apparently larger than that of the other components, and there is almost no record of an E-W component, which is consistent with the movement characteristics in this stage. The dip of the sliding surface was around 21°; thus, the force of the U-D component has a similar shape to the N-S component in this stage, with values of approximately one-third. In the entire landslide, it was only during this stage that the sliding mass moved in this direction; thus, the maximum force of the N-S component appears in this stage.

The main depositional zone and the debris depositional zone are located inside the Tiejianggou valley, distributing from south to north; and the source zone is on the upper part of the cliff to the west (Fig. 1). The Tiejianggou valley and the strike of the cliff are almost parallel to each other, with a height difference of more than 600 m. The west slope of the Tiejianggou valley was the main area in which the energy was released. During the second stage, the sliding mass scoured the west wall, forming the scouring zone, and the mass slid eastward along the west slope of the Tiejianggou valley, covering the maximum height difference of the entire event, releasing the majority of the energy, and finally colliding with the east slope of the valley. The mass broke up into small pieces, and flowed along the valley, forming the main depositional zone and the debris depositional zone (see Stage 2 in Fig. 1). The estimated source time functions show that the maximum force of the second stage appears in the E-W component; the eastward and the westward each reaches a peak, corresponding to the acceleration of the mass along the west slope, and the collision with the east slope, respectively. By comparison, the force of the N-S component was much smaller, indicating that no major movement occurred in this direction. The force of the E-W component during this stage was also the largest over the entire event, indicating that the movement in the E-W direction mainly occurred in this stage. As the mass moved along the west slope of the Tiejianggou valley, the U-D component also recorded a force with a shape similar to that of the E-W component; only the values are approximately half. Considering only the U-D

component, the maximum force appeared during this stage, indicating the maximum height difference along the path of the landslide. The source time functions of both the E-W component and the U-D component reach their maximum values in this stage, with magnitudes much larger than those of the N-S component in the first stage, indicating that the majority of the energy was released during this stage.

Tiejianggou is a long, narrow, and closed, inclined guide valley. The sliding mass did not stop immediately after the collision, but oscillated between the two banks of the valley and flowed downstream along the valley, expending its previously collected kinetic energy. Energy and material gathered within the valley and had no means of diffusion, which was one reason for the major scale of the disaster. Special geological and topographic conditions can have a focusing effect on landslides and are key factors in transforming them into major disasters. The spatial range of this stage is depicted in Fig. 1. The process is represented by the characteristics of the estimated source time functions in the E-W component, with peaks appearing alternately eastward and westward. No apparent force could be detected in the U-D component, indicating the negligible height difference along the Tiejianggou valley.

Dynamic history of the landslide

Topographic observations before and after the landslide reveal that the volume of the sliding mass was approximately 5×10^6 m^3 (Xu et al. 2009); and the total mass is estimated to be 1.15×10^{10} kg, assuming a density of 2.3×10^3 kg/m^3. The acceleration of the sliding mass could be calculated by dividing the inertial force by the total mass, and the velocity is the integral of the acceleration over time. The absolute velocities are shown in Fig. 6a, showing two peaks in each stage. The peaks in the first stage represent accelerations after the initiation, and after the failure of the key block, respectively, with values of approximately 10 m/s. The average velocity during this stage was 6.5 m/s. The two peaks in the second stage represent the accelerations when the sliding mass rushed down the west slope of the Tiejianggou valley, with an average velocity of 20.3 m/s, and a maximum velocity of approximately 35 m/s at approximately 130 s, before the collision with the east slope. The two peaks in the third stage represent oscillations of the sliding mass when flowing along the Tiejianggou valley, representing oscillation between the boundaries of the valley. The mean velocity of the sliding mass during this stage was approximately 13.8 m/s.

Taking the sliding mass as an ideal sliding block, the force acting on it could be expressed as:

$$f = mg(\sin\theta - \mu\cos\theta)$$

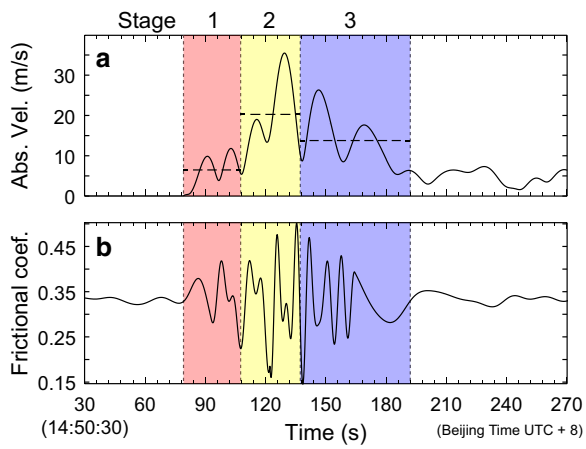

Fig. 6 **a** The absolute velocity of the sliding body, with average velocities of the three stages also depicted using *dashed lines*; and **b** the basal friction coefficients

where f is the force, m is the mass, g is the gravitational acceleration, θ is the angle of the slope, and μ is the basal friction coefficient. The basal friction coefficient could be calculated using the equation above, under the condition that the other parameters are known. The slope angle of the sliding path was approximately 18° according to field investigations. The inertial forces are projected onto the sliding path, and the friction coefficients calculated, as shown in Fig. 6b.

Basal friction coefficients exhibit the following characteristics: for the first stage, the values are relatively small, oscillating between 0.17 and 0.41, indicating the weak and thin layer along which the sliding surface developed. For the second stage, the sliding mass ran down the west slope of the Tiejianggou valley until it collided with the east slope. During this stage, the sliding mass scoured the sediment and bedrock at the foot of the cliff and flowed over the Tiejianggou valley; thus, the friction coefficient changed considerably, between 0.15 and 0.5. The friction coefficient was big when the sliding mass scoured the underlying materials, and it was small when it was flowing over the valley. During the third stage, the friction coefficient gradually decreased to a stable value of approximately 0.35, showing the characteristics of a debris flow.

We integrated the velocities once over time to acquire the displacements of the sliding mass, as shown in Fig. 7. The Wulong landslide was more complicated than ordinary landslides. After rushing down the west band of the Tiejianggou valley, the siding mass collided with the east bank of the valley and rebounded. This process can be clearly observed in Fig. 7. The run-out distance of the sliding mass is around 600 m, which is shorter than the field observation (Xu et al. 2009): because the inversion

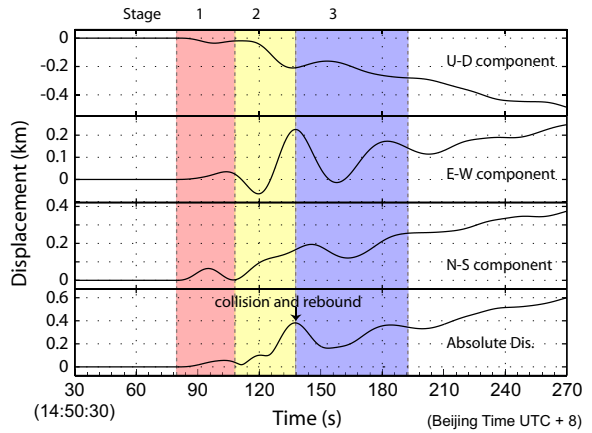

Fig. 7 Estimated displacements of the U-D component, E-W component, and N-S component; and the absolute displacement calculated from these three components

treated the source as a time-varying point, the run-out distance is only for the center of the mass, and does not cover the total range of the debris.

Conclusions

Massive landslides are catastrophic natural hazards. Research on the development and occurrence of landslides is very important for providing early warnings and for disaster prevention. In this paper, long-period seismic signals from 8 broadband seismic stations within 250 km of the Wulong landslide were selected for inversion to obtain their source time functions. Combining this data with that from topographic surveys, we conclude:

1. The Wulong landslide consisted of three stages: the initial stage occurred on the cliff from 80 to 108 s. The sliding mass moved from south to north. The second stage lasted from 108 to 137 s, moving eastward along the west slope of the Tiejianggou valley. The third stage was the debris flow after the collision with the east slope of the Tiejianggou valley, lasting from 137 to 192 s. The division of these three stages fits the topography very well. The kinetic energy of the landslide was mainly provided by the height difference between the source zone and depositional zones. The shape of the Tiejianggou Valley controlled the movement characteristics of the key stage of the landslide, i.e., the second stage. The collision between the sliding mass and the east slope of the Tiejianggou Valley not only changed the movement direction, but also broke up the mass into small pieces, forming the debris flow and changing the movement characteristics. Tiejianggou is a long, narrow, and closed, inclined guide valley. Debris frequently collided with the boundaries of the valley while flowing. Energy and material gathered within the valley, with no way of diffusing, leading to a major disaster. Special geological and topographic conditions had a significant effect on the disaster caused by the landslide.
2. The acceleration and velocity of the sliding mass were estimated using the total mass derived from topographic observations before and after the landslide. The average velocities of the sliding mass in the three stages were 6.5, 20.3, and 13.8 m/s, respectively. The maximum velocity was approximately 35 m/s, appearing before the end of the second stage.
3. The basal friction coefficient was also calculated, combined with the slope angle of the sliding path. The friction coefficient was relatively small in the first stage due to the thin weak layer; then changed a lot in the second stage due to variations in the topography; and gradually decreased to a stable value of approximately 0.35 in the third stage.

Our results show that long-period seismic signals can provide useful information for research on massive landslides. Quantitative research on landslides, using broadband seismic signals, is an effective tool for understanding their intrinsic processes.

Additional files

Additional file 1: Figure S1. The photo of the source region of the landslide, showing the locations of the key block, the stable bedrock and the loose material.

Additional file 2: Figure S2. The photo taken after the landslide, proving that the sliding mass broke up into small pieces after the collision with the east bank of the Tiejianggou valley.

Additional file 3: Figure S3. Amplitude spectrum of the three components of the WUL station in the low frequency part, helping to determine the frequency band used in the inversion.

Authors' contributions

ZL, XH and QX discussed and determined the overall framework of this study; DY, JF, and XQ prepared the seismic data and conducted field investigations; and XH processed the seismic data and prepared the manuscript with contributions from all the co-authors. All authors read and approved the final manuscript.

Author details

[1] China Earthquake Networks Center, Beijing 100045, China. [2] State Key Laboratory of Geohazard Prevention and Geoenvironment Protection, Chengdu University of Technology, Chengdu 610059, China. [3] Institute of Seismology, China Earthquake Administration, Wuhan 430071, China.

Acknowledgements

We would like to thank Liu Ruifeng, Huang Zhibin, and Zhao Yong from the China Earthquake Networks Center for their helpful comments on seismic wave recognition. We also thank Ma Yanlu and Zhao Xu from the China Earthquake Networks Center for their helpful comments on the calculation of Green's Functions. The velocity model used in the inversion is from Crust1.0; RDSEED and SAC were used in seismic data processing. This research was financially supported by the National Basic Research Program "973" project

of the Ministry of Science and Technology of the People's Republic of China (2013CB733200). We would like to extend special thanks to two anonymous reviewers for their valuable suggestions, which greatly improved the quality of this paper.

Competing interests
The authors declare that they have no competing interests.

Received: 9 August 2016 Accepted: 24 January 2017
Published online: 03 February 2017

References

Allstadt K (2013) Extracting source characteristics and dynamics of the August 2010 Mount Meager landslide from broadband seismograms. J Geophys Res 118:1472–1490. doi:10.1002/jgrf.20110

Ekström G, Stark CP (2013) Simple scaling of catastrophic landslide dynamics. Science 339:1416–1419. doi:10.1126/science.1232887

Hibert C, Ekström G, Stark CP (2014) Dynamics of the Bingham Canyon mine landslides from seismic signal analysis. Geophys Res Lett 41:4535–4541. doi:10.1002/2014GL060592

Hibert C, Stark C, Ekström G (2015) Dynamics of the Oso-Steelhead landslide from broadband seismic analysis. Nat Hazards Earth Syst Sci 15:1265–1273. doi:10.5194/nhess-15-1265-2015

Kanamori H, Given JW (1982) Analysis of long-period seismic waves excited by the May 18, 1980, eruption of Mount St. Helens—a terrestrial monopole? J Geophys Res 87:5422–5432. doi:10.1029/JB087iB07p05422

Kawakatsu H (1989) Centroid single force inversion of seismic waves generated by landslides. J Geophys Res 94:12363–12374. doi:10.1029/JB094iB09p12363

Lin C-H (2015) Insight into landslide kinematics from a broadband seismic network. Earth Planets Space 67:1–6. doi:10.1186/s40623-014-0177-8

Lin CH, Kumagai H, Ando M, Shin TC (2010) Detection of landslides and submarine slumps using broadband seismic networks. Geophys Res Lett 37:L22309. doi:10.1029/2010GL044685

Nakano M, Kumagai H, Inoue H (2008) Waveform inversion in the frequency domain for the simultaneous determination of earthquake source mechanism and moment function. Geophys J Int 173:1000–1011. doi:10.1111/j.1365-246X.2008.03783.x

Petley DN (2013) Characterizing giant landslides. Science 339:1395–1396. doi:10.1126/science.1236165

Wang R (1999) A simple orthonormalization method for stable and efficient computation of Green's functions. Bull Seismol Soc Am 89:733–741

Xu Q, Huang R, Yin Y, Hou S, Dong X, Fan X, Tang M (2009) The Jiweishan landslide of June 5, 2009 in Wulong, Chongqing: characteristics and failure mechanism. J Eng Geol 17:433–444 **(in Chinese)**

Yamada M, Kumagai H, Matsushi Y, Matsuzawa T (2013) Dynamic landslide processes revealed by broadband seismic records. Geophys Res Lett 40:2998–3002. doi:10.1002/grl.50437

Yin Y (2010) Mechanism of apparent dip slide of inclined bedding rockslide: a case study of Jiweishan rockslide in Wulong, Chongqing. Chin J Rock Mech Eng 29:217–226 **(in Chinese)**

Zhao J, Moretti L, Mangeney A, Stutzmann E, Kanamori H, Capdeville Y, Calder ES, Hibert C, Smith PJ, Cole P, Lefriant A (2015) Model space exploration for determining landslide source history from long-period seismic data. Pure appl Geophys 172:389–413. doi:10.1007/s00024-014-0852-5